# LINEAR WAVE INTERACTION WITH A VERTICAL CYLINDER OF ARBITRARY CROSS SECTION. ASYMPTOTIC APPROACH

N.B. Dişibüyük [1], A.A. Korobkin [2] and O. Yılmaz [3]

## ABSTRACT

An asymptotic approach to the linear problem of regular water waves interacting with a vertical cylinder of arbitrary cross section is presented. The incident regular wave is one-dimensional, water is of finite depth, and the rigid cylinder extends from the bottom to the water surface. The non-dimensional maximum deviation of the cylinder cross section from a circular one plays the role of a small parameter of the problem. A fifth-order asymptotic solution of the problem is obtained. The problems at each order are solved by the Fourier method. It is shown that the first-order velocity potential is a linear function of the Fourier coefficients of the shape function of the cylinder, the second-order velocity potential is a quadratic function of these coefficients, and so on. The hydrodynamic forces acting on the cylinder and the water surface elevations on the cylinder are presented. The comparisons of the present asymptotic results with numerical and experimental results of previous investigations show good agreement. Long wave approximation of the hydrodynamic forces is derived and used for validation of the asymptotic solutions. The obtained values of the forces are exact in the limit of zero wave numbers within the linear wave theory. An advantage of the present approach compared with the numerical solution of the problem by an integral equation method is that it provides the forces and the diffracted wave field in terms of the coefficients of the Fourier series of the deviation of the cylinder shape from the circular one. The resulting asymptotic formula can be used for optimization of the cylinder shape in terms of the wave loads and diffracted wave fields.

**Keywords:** Linear water waves, non-circular vertical cylinder, asymptotic analysis, wave loads.

## INTRODUCTION

Prediction of wave forces is important to engineers for the design of offshore and coastal structures. Floating airports, bridge pylons, semi submersibles, Tension Leg platforms are typical examples of such structures. For large scale structures, one should take the diffraction effects into account. The potential wave theory is usually used to estimate the wave loads.

The wave body interaction is a three dimensional and nonlinear problem with unknown in advance position of the free surface of the liquid and unknown wetted surface of the

[1] Ph.D. Student and Research Assistant, Department of Mathematics, Dokuz Eylul University, Tnaztepe Campus, 35390, Buca, Izmir, Turkey (corresponding author). E-mail: bugurcan.ruzgar@deu.edu.tr

[2] Professor, School of Mathematics, University of East Anglia, Norwich, NR4 7TJ, UK. E-mail: a.korobkin@uea.ac.uk

[3] Professor, Department of Mathematics, Izmir Institute of Technology, 35430, Urla, Izmir, Turkey. E-mail: oguzyilmaz@iyte.edu.tr

body. The problem can be linearized for waves of small amplitude compared with the water depth, wave length, and linear size of the body. Within the linear theory of water waves we linearize the free surface boundary conditions and impose them on the equilibrium level of water surface. Viscous effects and surface tension of the liquid are important for short water waves with relatively high frequency. For large dimensions of offshore structures and moderate wave length, both viscous and capillary effects can be neglected at leading order. The resulting linear problem of wave theory is additionally simplified if the water depth is constant and the structure is a vertical cylinder extending from the flat sea bottom to the free surface. Such cylinders represent legs of offshore platforms and piles of offshore wind turbines. Offshore platforms are used for exploration of oil and gas from under seabed and processing. A general offshore structure has a deck which is supported by deck legs. The hydrodynamic forces acting on these legs are of major concern to engineers because the design of the legs is dominated by wave loads. In many applications, the cylinders are of circular cross sections but not necessarily.

One of the first studies of diffraction of plane water waves by stationary obstacles with vertical sides was done by Havelock (1940) for water of infinite depth. Results were obtained for cylinders of circular and parabolic sections. Cylinders of ship forms were also studied by Havelock using some approximations with applications to a ship advancing in waves. The draught of the ship was assumed infinite. Havelock (1940) noticed that for periodic linear water waves and obstacles with vertical sides both time and the vertical coordinate can be separated from the problem and the original problem of water waves can be reduced to the two-dimensional problem of plane sound waves diffracted by the two-dimensional rigid body representing the cross section of the vertical cylinder. Then known results from diffraction problems of sound and electromagnetic waves can be transferred and applied to the problem of water waves diffracted by a vertical cylinder. MacCamy and Fuchs (1954) extended this approach to water of finite constant depth and a surface piercing vertical circular cylinder.

Chen and Mei (1971) solved the water wave diffraction problem for vertical elliptic cylinder. The elliptic cylindrical coordinates and the method of separating variables were used to find the velocity potential in terms of infinite series of Mathieu functions. In another study, Chen and Mei (1973) investigated the same problem using long wave approximation. Numerical results were also presented for a shiplike body. Williams (1985) used two different methods to solve the diffraction problem for elliptic vertical cylinders. One method employed the two-terms asymptotic expansions of the exact solution for the forces and moments acting on the elliptic cylinder with small eccentricity. The second method is the integral equation method. It was concluded that the asymptotic method gives good results for small wave numbers. In a very recent study by Liu et al. (2016), wave diffraction by a uniform bottom mounted cylinder of arbitrary cross section was numerically studied. The velocity potential was sought in the form suggested by MacCamy and Fuchs (1954) for a circular cylinder. However now the coefficients in the Fourier series for diffracted waves were determined by using the body boundary condition for the non-circular cylinder. In this numerical method, the body boundary condition was satisfied approximately by the Galerkin method. Fourier series were used to represent the cross sections of the cylinders and the free surface elevation. As a practical application of this numerical method, the wave forces and wave runup on quasi-elliptic caisson foundations of a cross-strait bridge pylon were investigated. These numerical results are used in the present paper for validation of our asymptotic solutions.

There are two main approaches to the numerical treatment of the diffraction problem of cylinders with arbitrary cross section. One of them is the integral equation method developed by Hwang and Tuck (1970) in the investigation of harbor resonance. Isaacson (1978) applied this method to calculations of wave forces on cylinders used in offshore structures. The method is based on source or source-dipole distribution and Green's theorem. The resulting Fredholm integral equation of the second kind for the velocity potential is solved by discretizing the cylinder contour into small segments. This method was also used by Mansour et al. (2002) and Wu and Price (1991). Wu and Price (1991) calculated wave drift forces acting on multiple vertical cylinders of arbitrary cross sections. The boundary element method was developed by Au and Brebbia (1983) for the diffraction problem of vertical cylinders. This method is based on the Galerkin weighted residual formulation. After obtaining the integral equation, the boundary of the cylinder is discretized into boundary elements which are chosen to be either constant or linear or quadratic. The boundary element method was applied to the cylinders of circular, elliptic and square cross sections. Au and Brebbia (1983) obtained the wave forces acting on a square cylinder and compared their results with the experimental and numerical results of Mogridge and Jamieson (1976). The agreement between the numerical, experimental and theoretical predictions of the hydrodynamic forces acting on the square cylinder was shown to be fairly good. Approximation of "equivalent circular radius" was used by Mogridge and Jamieson (1976). In this approximation, the horizontal hydrodynamic force acting on a vertical cylinder is approximated by the force acting on the circular cylinder of the same area of its cross section. The boundary element method of Au and Brebbia (1983) was used by Zhu and Moule (1994) in the problem of short crested wave interaction with vertical cylinders of arbitrary cross section. The boundary element method for the diffraction problem of vertical and horizontal cylinders is explained in detail by Wrobel et al. (1985).

The numerical methods such as the integral equation method and the boundary element method could be used to solve the diffraction problem for vertical cylinders of arbitrary section. However, in some cases these numerical methods are not preferable, for example in evaluating free surface integrals in the second order diffraction problem of vertical cylinders (see Eatock Taylor and Hung (1987)). The free surface integral converges slowly and the values of the first order potential have to be evaluated many times, which is not possible by the integral equation methods. Also the integral equation methods require quite fine discretization of the boundary of the cylinder, which could be tedious and is the source of errors. The method of the present paper, which was originally proposed by Mei et al. (2005), can deal with geometries of arbitrary cross section with little effort.

In this paper, the linear water waves scattering by a vertical cylinder with arbitrary cross section extending from the sea bottom to the free surface in water of finite depth are studied by asymptotic methods. The non-dimensional maximum deviation of the cylinder cross section from a circular one plays the role of a small parameter of the problem. A fifth-order asymptotic solution of the problem is obtained. Numerical calculations of the diffracted velocity potential, the forces acting on the cylinder and the diffracted wave field are reduced to operations with the Fourier coefficients of the shape function, which describes the cross section of the cylinder, and the velocity potentials on the cylinder surface at each order of approximation. It is shown that the first-order velocity potential is a linear function of the Fourier coefficients of the shape function of the cylinder, the second-order velocity potential is a quadratic function of these coefficients, and so on. The obtained solution makes it possible to formulate and solve two practical problems in terms of the Fourier coefficients of the shape function: optimization of the shape of the cylinder and identification of the cylinder shape by using measured wave field far from the cylinder. The asymptotic approach of this paper is applied to calculations of the hydrodynamic forces acting on elliptic, quasi-elliptic, and square cylinders. The comparisons of the asymptotic forces with available numerical and experimental results by others demonstrate good accuracy of the present approach. Long-wave approximation of the hydrodynamic forces is obtained and used for validation of the asymptotic solution.

Note that Mei et al. (2005) were concerned with the leading order corrections to the forces caused by small deviation of a vertical elliptic cylinder from the circular one. A similar perturbation approach was used by Mansour et al. (2002) for vertical cylinders with a cosine type radial perturbation of the cylinder cross section. The leading order corrections to the forces were obtained and compared to the numerical results by the integral equation method. It was shown that the agreement is good for small perturbation amplitude. In contrast to the perturbation analysis by Mansour et al. (2002), our asymptotic approach is not restricted to a particular shape of cylinders and a fifth-order approximation of the solution is obtained. It will be shown in this paper that the fifth-order asymptotic solution makes it possible to consider even such "non-circular" cylinders as square ones and obtain accurate results in terms of the hydrodynamic forces.

The present asymptotic approach can be extended to truncated vertical cylinders and oscillating rigid and elastic cylinders of arbitrary cross sections, as well as to submerged horizontal cylinders in plane incident waves. The diffraction problem of a truncated vertical cylinder of circular cross section of radius $a$ was solved by Garrett (1971). In his paper, both the incident and diffracted waves were expanded in Bessel functions in the interior region ($r < a$) and in the exterior region ($r > a$) and then these two solutions and the derivatives of the solutions were matched at the boundary ($r = a$). Black et al. (1971) used a variational formulation and a theorem due to Haskind to calculate wave forces on a stationary body using only far field properties. Yeung (1981) used the same method to solve the radiation problem for a truncated vertical cylinder of circular cross section. In the case of deep water, the multipole expansions are usually convenient to describe the velocity potential for wave diffraction and radiation. Ursell (1950) used a series of complex potential functions arising from multipoles at the center of the cylinder to solve the problem of the generation of surface waves by a submerged circular cylinder. Thorne (1953) investigated the motion arising from line and point singularities using multipole expansion method in deep and shallow waters. Two-dimensional multipoles were developed in a systematic way for submerged and floating cylinders by Eatock Taylor and Hu (1991). The application to arbitrary body shapes was made by coupling the multipole expansion with a boundary integral method.

The outline of the paper is as follows: mathematical formulation of the problem and its solution for a vertical circular cylinder are given in the next section. The fifth-order asymptotic solution of the problem is described in section "Vertical Cylinders With Nearly Circular Cross Section". Each approximation of this asymptotic solution is obtained by operating with the Fourier coefficients of the shape function and the velocity potentials of the lower order approximations. The asymptotic approach is applied to elliptic cylinders in waves and the obtained results are compared with numerical results of Williams (1985) in section "Hydrodynamic Force on Elliptic Vertical Cylinder". In the next section, the present approach is applied to square cylinders and the obtained results are compared with experimental results by Mogridge and Jamieson (1976) in terms of the horizontal forces acting on square cylinders. In section "Hydrodynamic Force on Quasi-Elliptic Vertical Cylinder" the results of the present asymptotic method are compared with the three-dimensional solution of the Navier-Stokes equations by Wang et al. (2011). The wave force and runup values for cylinders with circular, elliptic, quasi-elliptic and square cross sections with the same cross sectional area are compared. In the next section, the wave force and wave runup on cylinders with cosine type perturbations of their cross sections are studied and compared with the numerical results by Mansour et al. (2002) and Liu et al. (2016). Asymptotic behavior of wave forces for long waves is studied in section "Long Wave Approximation of Wave Forces" for cylinders with arbitrary cross sections. The findings of the analysis are summarized and conclusions are drawn in the last section of this paper.

## FORMULATION OF THE PROBLEM

Diffraction of two-dimensional water waves by a vertical cylinder of almost circular cross section is studied within the linear wave theory. The problem is formulated in a polar coordinate system $(r, \theta, z)$ where the $z$ axis points vertically upwards. The plane $z = -h$ corresponds to the sea bottom and the plane $z = 0$ corresponds to the mean level of water surface. The rigid cylinder extends from the sea bottom to the free surface. The cross

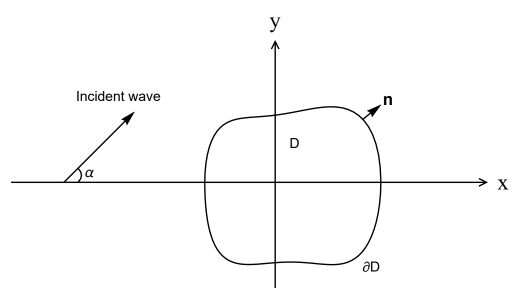


FIG. 1: Top view of the problem configuration.

section of the vertical cylinder is described by the equation $r = R[1 + \varepsilon f(\theta)]$, where $R$ is the mean radius of the cylinder and $\varepsilon$ is a small non-dimensional parameter of the problem. The top view of the studied configuration is shown in Figure 1. The smooth and bounded function $f(\theta)$ describes the deviation of the shape of the cylinder from the circular one. A one-dimensional incident wave of amplitude $A$ and wave frequency $\omega$ propagates at angle $\alpha$ to the positive $x$-axis from $x \sim -\infty$ towards the cylinder. Within the linear wave theory (see Mei et al. (2005)), the wave field is described by a velocity potential $\Phi(r, \theta, z, t)$. For a vertical cylinder of arbitrary cross section the velocity potential is expressed only through the propagating wave mode,

$$\Phi(r, \theta, z, t) = \mathrm{Re}\left\{ \frac{gA}{\omega} \frac{\cosh[k(z+h)]}{\cosh(kh)} \phi(r, \theta) e^{-i\omega t} \right\}, \tag{1}$$

where $i = \sqrt{-1}$ and $\mathrm{Re}\{\mathscr{A}\}$ denotes the real part of a complex number $\mathscr{A}$. The complexvalued function $\phi(r,\theta)$ satisfies the Helmholtz equation,

$$\phi_{rr} + \frac{1}{r}\phi_r + \frac{1}{r^2}\phi_{\theta\theta} + k^2\phi = 0 \quad (r > R[1+\varepsilon f(\theta)]), \tag{2}$$

in the flow region, the far-field condition,

$$\phi \sim e^{ikr\cos(\theta-\alpha)} \quad (r \to \infty), \tag{3}$$

and the boundary condition on the surface of the cylinder,

$$\frac{\partial \phi}{\partial n} = 0 \quad (r = R[1+\varepsilon f(\theta)]). \tag{4}$$

Here $\mathbf{n}$ is the unit outward normal vector to the surface of the cylinder, $g$ is the gravitational acceleration, $k$ is the wave number, $k = 2\pi/\lambda$, $\lambda$ is the length of the incident wave. The wave number $k$ is related to the wave frequency $\omega$ by the dispersion relation $\omega^2 = gk\tanh(kh)$, $k > 0$.

The hydrodynamic force $\mathbf{F}(t) = (\mathcal{F}_x, \mathcal{F}_y)$, acting on the vertical cylinder is obtained by integration of the dynamic pressure, $p(r,\theta,z,t) = -\rho\,\partial\Phi/\partial t$, over the wetted part of the cylinder

$$\mathbf{F}(t) = -\int_{-h}^{0}\int_{\partial D} p\,\mathbf{n}\,\mathrm{d}s\,\mathrm{d}z = -\rho g A \frac{\tanh(kh)}{k}\,\mathrm{Re}\left\{ i \int_{\partial D} \phi(r,\theta)\,\mathbf{n}\,\mathrm{d}s\, e^{-i\omega t}\right\}, \tag{5}$$

where $\partial D$ is the boundary of the cylinder cross section, $r = R[1+\varepsilon f(\theta)]$, and $\mathrm{d}s$ is a small element of this boundary. The non-dimensional force scaled with $\rho g A \pi a^2 \tanh(kh)$ is denoted by tilde. Here $a$ is a characteristic dimension of the vertical cylinder cross section, which can be different from $R$. The components of the non-dimensional force are given by

$$\tilde{\mathcal{F}}_x(t) = \mathrm{Re}\{\tilde{F}_x\, e^{-i\omega t}\}, \quad \tilde{\mathcal{F}}_y(t) = \mathrm{Re}\{\tilde{F}_y\, e^{-i\omega t}\}, \tag{6}$$

$$\tilde{F}_x = \frac{-iR}{\pi k a^2}\int_0^{2\pi} \phi(R[1+\varepsilon f(\theta)],\theta)[\varepsilon f'(\theta)\sin\theta + [1+\varepsilon f(\theta)]\cos\theta]\ \mathrm{d}\theta, \tag{7}$$

$$\tilde{F}_y = \frac{-iR}{\pi k a^2}\int_0^{2\pi} \phi(R[1+\varepsilon f(\theta)],\theta)[-\varepsilon f'(\theta)\cos\theta + [1+\varepsilon f(\theta)]\sin\theta]\ \mathrm{d}\theta. \tag{8}$$

Note that the phases of $\tilde{F}_x$ and $\tilde{F}_y$ depend on the position of the origin $O$ of the coordinate system, see Figure 1, but the modulus $|\tilde{F}_x|$ and $|\tilde{F}_y|$ are independent of the coordinate system.

The elevation of the free surface, $z = \eta(r,\theta,t)$, is related to the unknown potential $\phi(r,\theta)$ by the linear kinematic boundary condition, $\eta_t = \Phi_z(r,\theta,0,t)$, which gives

$$\eta(r,\theta,t) = \mathrm{Re}\{iA\,\phi(r,\theta)\,e^{-i\omega t}\}. \tag{9}$$

The far-field condition (3) and equation (9) provide the assumed shape of the incident wave $\eta_I(r,\theta,t)$:

$$\eta_I(r,\theta,t) = A\sin(\omega t - kr\cos(\theta-\alpha)), \tag{10}$$

with $\eta_I(0,\theta,t) = A\sin(\omega t)$ at the origin of the coordinate system.

The maximum elevation of the water surface at the cylinder per the wave period is known as the wave runup, $\triangle(\theta)$. The wave runup is scaled in this paper with the wave height, $2A$. Equation (9) yields $\triangle(\theta)/2A = |\phi(r,\theta)|/2$, where $r = R[1+\varepsilon f(\theta)]$. The wave runup and its dependence on the shape of the cylinder are important in design of offshore structures, where the wave runup should not exceed the elevation of the wetdeck of an offshore structure above the mean water level. Wave runup on offshore structures could be much higher than that predicted by the linear wave theory, see De Vos et al. (2007), Lykke Andersen et al. (2011). Nonlinear waves with steep front or breaking in front of the structure produce thin runup sheet and spray near the structure increasing the runup. The runup can be also affected by aeration of water near the structure due to the wave breaking, in particular. Many nonlinear physical effects near the structure are not included in the present linear model. However, it can be shown that these effects provide small contributions to the hydrodynamic structure (Iafrati and Korobkin (2006), Korobkin and Malenica (2007), Korobkin (2008)) and the diffracted wave field.

The problem (2)-(4) for arbitrary vertical cylinder can be solved only numerically. The analytical solution is well known for the circular cylinder, $r = R$, see MacCamy and Fuchs (1954). This solution corresponds in this study to the leading-order velocity potential of the problem (2)-(4) as $\varepsilon \to 0$,

$$\phi_0(r,\theta) = \sum_{m=0}^{\infty} \epsilon_m i^m \left[ J_m(kr) - \frac{J_m'(kR)}{H_m^{(1)'}(kR)} H_m^{(1)}(kr) \right] \cos[m(\theta-\alpha)], \tag{11}$$

where $\epsilon_m$ is the Neumann symbol, $\epsilon_0 = 1$, $\epsilon_m = 2$ for $m \geq 1$, $J_m(r)$ are the Bessel functions of the first kind with order $m$, $H_m^{(1)}(r)$ are the Hankel functions of the first kind corresponding to outward-propagating cylindrical waves, prime stands for derivatives with respect to the argument. By using the Wronskian identity, $J_m(r)H_m^{(1)'}(r) - J_m'(r)H_m^{(1)}(r) = 2i/(\pi r)$, the potential $\phi_0(r,\theta)$ on the surface of the cylinder is given by

$$\phi_0(R,\theta) = \frac{2i}{\pi kR} \sum_{m=0}^{\infty} \frac{\epsilon_m i^m}{H_m^{(1)'}(kR)} \cos[m(\theta-\alpha)]. \tag{12}$$

Here

$$\frac{2i}{\pi\, kR\, H_m^{(1)'}(kR)} \sim \sqrt{\frac{2}{\pi m}} e^{-m\,\log\left(\frac{2m}{ekR}\right)} \tag{13}$$

as $m \to \infty$. Therefore, the series (12) converges exponentially and only a few terms are needed to calculate the potential $\phi_0(R,\theta)$ and its derivatives in $\theta$ with good accuracy.

Equations (12) and (7) provide the total non-dimensional hydrodynamic force acting on the circular cylinder in the incident regular wave with $\alpha = 0°$ and $a = R$ (see Mei et al. (2005))

$$\tilde{F}_x = \frac{4i}{\pi (kR)^2 H_1^{(1)'}(kR)}. \tag{14}$$

We shall determine the force formula similar to (14) for $\varepsilon > 0$ and a given function $f(\theta)$ describing the cross section of a non-circular vertical cylinder.

## VERTICAL CYLINDERS WITH NEARLY CIRCULAR CROSS SECTIONS

Asymptotic methods are used to find an approximate solution of the problem (2)-(4) as $\varepsilon \to 0$. The derivatives $\partial\phi/\partial\theta$ and $\partial\phi/\partial r$ in the boundary condition (4) on the surface of the cylinder,

$$\frac{\partial\phi}{\partial r}(R[1+\varepsilon f(\theta)],\theta) - \frac{\varepsilon f'(\theta)}{R[1+\varepsilon f(\theta)]^2}\frac{\partial\phi}{\partial\theta}(R[1+\varepsilon f(\theta)],\theta) = 0,$$

are approximated by their Taylor series up to $\mathcal{O}(\varepsilon^5)$ at $r = R$ and then the fifth order asymptotic expansion of the potential $\phi(r,\theta)$,

$$\phi(r,\theta) = \phi_0(r,\theta) + \varepsilon\phi_1(r,\theta) + \varepsilon^2\phi_2(r,\theta) + \varepsilon^3\phi_3(r,\theta) + \varepsilon^4\phi_4(r,\theta) + \mathcal{O}(\varepsilon^5), \tag{15}$$

is substituted in the boundary condition. The resulting approximation of the condition (4) is

$$\begin{aligned}
&\phi_{0,r} + \varepsilon\Big[\phi_{1,r} + Rf(\theta)\phi_{0,rr} - \frac{f'(\theta)}{R}\phi_{0,\theta}\Big] \\
&\quad + \varepsilon^2\Big[\phi_{2,r} + Rf(\theta)\phi_{1,rr} - \frac{f'(\theta)}{R}\phi_{1,\theta} + \frac{R^2f^2(\theta)}{2}\phi_{0,rrr} + \frac{2f(\theta)f'(\theta)}{R}\phi_{0,\theta} - f(\theta)f'(\theta)\phi_{0,r\theta}\Big] \\
&\quad + \varepsilon^3\Big[\phi_{3,r} + Rf(\theta)\phi_{2,rr} - \frac{f'(\theta)}{R}\phi_{2,\theta} + \frac{R^2f^2(\theta)}{2}\phi_{1,rrr} + \frac{2f(\theta)f'(\theta)}{R}\phi_{1,\theta} - f(\theta)f'(\theta)\phi_{1,r\theta} \\
&\qquad\quad + 2f^2(\theta)f'(\theta)\phi_{0,r\theta} + \frac{R^3f^3(\theta)}{6}\phi_{0,rrrr} - \frac{3f^2(\theta)f'(\theta)}{R}\phi_{0,\theta} - \frac{Rf^2(\theta)f'(\theta)}{2}\phi_{0,rr\theta}\Big] \\
&\quad + \varepsilon^4\Big[\phi_{4,r} + Rf(\theta)\phi_{3,rr} - \frac{f'(\theta)}{R}\phi_{3,\theta} + \frac{R^2f^2(\theta)}{2}\phi_{2,rrr} - f(\theta)f'(\theta)\phi_{2,r\theta} + \frac{2f(\theta)f'(\theta)}{R}\phi_{2,\theta} \\
&\qquad\quad - \frac{3f^2(\theta)f'(\theta)}{R}\phi_{1,\theta} - \frac{Rf^2(\theta)f'(\theta)}{2}\phi_{1,rr\theta} + 2f^2(\theta)f'(\theta)\phi_{1,r\theta} + \frac{R^3f^3(\theta)}{6}\phi_{1,rrrr} \\
&\qquad\quad - 3f^3(\theta)f'(\theta)\phi_{0,r\theta} + Rf^3(\theta)f'(\theta)\phi_{0,rr\theta} - \frac{R^2f^3(\theta)f'(\theta)}{6}\phi_{0,rrr\theta} + \frac{R^4f^4(\theta)}{24}\phi_{0,rrrrr} \\
&\qquad\quad + \frac{4f^3(\theta)f'(\theta)}{R}\phi_{0,\theta}\Big] = \mathcal{O}(\varepsilon^5),
\end{aligned} \tag{16}$$

where the functions $\phi_n(r,\theta)$ and their derivatives are calculated at $r = R$. At the leading order as $\varepsilon \to 0$, condition (16) provides $\phi_{0,r}(R,\theta) = 0$. This is the boundary condition which leads to the solution (11) for the circular cylinder. At the first order, condition (16) gives

$$\phi_{1,r}(R,\theta) = \frac{f'(\theta)}{R}\phi_{0,\theta}(R,\theta) - Rf(\theta)\phi_{0,rr}(R,\theta). \tag{17}$$

The unknown potentials $\phi_n(r,\theta)$, $n = 0,1,2,3,4$, in (15) satisfy equation (2). This equation is used, in particular, to calculate the second derivative $\phi_{0,rr}$ and to write (17) in terms of $\phi_0(R,\theta)$ given by (12) and its derivatives in $\theta$:

$$\phi_{1,r}(R,\theta) = \frac{1}{R}f(\theta)\phi_{0,\theta\theta} + \frac{1}{R}f'(\theta)\phi_{0,\theta} + R\,k^2f(\theta)\phi_0(R,\theta). \tag{18}$$

Note that the wave number $k$ now appears in the boundary condition for the potential $\phi_1(r,\theta)$.

Equating the terms in (16) with $\varepsilon^2$, $\varepsilon^3$ and $\varepsilon^4$ to zero, the boundary conditions for the potentials $\phi_2$, $\phi_3$ and $\phi_4$ are obtained respectively. These boundary conditions have the form $(n = 1, 2, 3, 4)$

$$\phi_{n,r}(R, \theta) = G_n(\theta), \tag{19}$$

where $G_n(\theta)$ are the sums of the products of the functions $f(\theta)$, $f'(\theta)$, $\phi_0(R, \theta)$,..., $\phi_{n-1}(R, \theta)$ and derivatives of the potentials $\phi_0(R, \theta)$,..., $\phi_{n-1}(R, \theta)$ in $\theta$. Starting from the solution (12) for the circular cylinder and a given function $f(\theta)$, we calculate the right-hand side, $G_1(\theta)$, in (18) and then determine the outward-propagating wave solution, $\phi_1(r, \theta)$, of equation (2) subject to the boundary condition (18) on the circular cylinder, $r = R$. By using the obtained potential $\phi_1(r, \theta)$, we calculate $G_2(\theta)$ and determine $\phi_2(r, \theta)$, and so on. The boundary value problems for the potentials $\phi_n(r, \theta)$ are identical and differ only by functions $G_n(\theta)$ in the body boundary condition (19). By using the Fourier series of the functions $G_n(\theta)$,

$$G_n(\theta) = \frac{1}{2} G_{n0}^{(c)} + \sum_{m=1}^{\infty} G_{nm}^{(c)} \cos(m\theta) + G_{nm}^{(s)} \sin(m\theta), \tag{20}$$

the potentials are given by

$$\phi_n(r, \theta) = \frac{1}{2} G_{n0}^{(c)} \frac{H_0^{(1)}(kr)}{k H_0^{(1)'}(kR)} + \sum_{m=1}^{\infty} [G_{nm}^{(c)} \cos(m\theta) + G_{nm}^{(s)} \sin(m\theta)] \frac{H_m^{(1)}(kr)}{k H_m^{(1)'}(kR)}. \tag{21}$$

In particular, $\phi_n(R, \theta)$ and their derivatives are obtained in the form of their Fourier series. Calculations of the functions $G_n(\theta)$ and their Fourier coefficients are reduced to multiplication and summation of Fourier series. If the coefficients in the Fourier series of the function $f(\theta)$ are known,

$$f(\theta) \sim \frac{f_0^{(c)}}{2} + \sum_{m=1}^{\infty} f_m^{(c)} \cos(m\theta) + f_m^{(s)} \sin(m\theta), \tag{22}$$

and using the Fourier series (12) of $\phi_0(R, \theta)$, we calculate the derivatives $f'(\theta)$, $\phi_{0,\theta}(R, \theta)$, $\phi_{0,\theta\theta}(R, \theta)$ by differentiating (12) and (22) term by term and then we can determine the Fourier coefficients of the right-hand side in (18). Finally the solution $\phi_1(r, \theta)$ is given by (21). Similar arguments are applied to the higher-order problems for $\phi_2$, $\phi_3$ and $\phi_4$. It is seen that the asymptotic solution (15) of the problem is obtained by operating with the Fourier coefficients of the potentials $\phi_n(R, \theta)$ and the function $f(\theta)$ which describe the shape of the vertical cylinder. Summation and differentiation of Fourier series are straightforward operations. The multiplication of two Fourier series,

$$g(\theta) \sim \frac{a_0}{2} + \sum_{m=1}^{\infty} a_m \cos(m\theta) + b_m \sin(m\theta),$$

$$h(\theta) \sim \frac{\alpha_0}{2} + \sum_{m=1}^{\infty} \alpha_m \cos(m\theta) + \beta_m \sin(m\theta),$$

provides the Fourier series

$$g(\theta)h(\theta) \sim \frac{A_0}{2} + \sum_{m=1}^{\infty} A_m \cos(m\theta) + B_m \sin(m\theta), \tag{23}$$

where (see Fichtenholtz (2001))

$$A_n = \frac{a_0\alpha_n}{2} + \frac{1}{2}\sum_{m=1}^{\infty} [a_m(\alpha_{m+n} + \alpha_{m-n}) + b_m(\beta_{m+n} + \beta_{m-n})], \tag{24}$$

$$B_n = \frac{a_0\beta_n}{2} + \frac{1}{2}\sum_{m=1}^{\infty} [a_m(\beta_{m+n} - \beta_{m-n}) - b_m(\alpha_{m+n} - \alpha_{m-n})], \tag{25}$$

$\beta_{m-n} = -\beta_{n-m}$ and $\alpha_{m-n} = \alpha_{n-m}$ if $m - n < 0$.

Calculations of the components $\tilde{F}_x$ and $\tilde{F}_y$ of the hydrodynamic force acting on the vertical cylinder and the diffracted waves far from the cylinder can also be reduced to operations with the Fourier coefficients of the function $f(\theta)$ and the potentials $\phi_n(R, \theta)$. For example, the integrand of $\tilde{F}_x$ in (7) can be approximated as

$$\phi(R[1 + \varepsilon f(\theta)], \theta)[\varepsilon f'(\theta) \sin\theta + [1 + \varepsilon f(\theta)] \cos\theta] = \sum_{n=0}^{4} \varepsilon^n S_n(\theta) + \mathcal{O}(\varepsilon^5),$$

where

$$S_n(\theta) = \frac{1}{2} S_{n0}^{(c)} + \sum_{m=1}^{\infty} [S_{nm}^{(c)} \cos(m\theta) + S_{nm}^{(s)} \sin(m\theta)].$$

The non-dimensional $x$-component of the force is given by

$$\tilde{F}_x = -\frac{iR}{ka^2} \left( S_{00}^{(c)} + \varepsilon S_{10}^{(c)} + \varepsilon^2 S_{20}^{(c)} + \varepsilon^3 S_{30}^{(c)} + \varepsilon^4 S_{40}^{(c)} \right) + \mathcal{O}(\varepsilon^5). \tag{26}$$

Here $S_{00}^{(c)}$ provides the force acting on the circular cylinder, $r = R$, $S_{10}^{(c)}$ is a linear function of the Fourier coefficients $f_m^{(c)}$ and $f_m^{(s)}$ in (22), and $S_{20}^{(c)}$ is a quadratic function of these coefficients. A similar analysis is applied to calculations of the $y$-component of the force, $\tilde{F}_y$.

Far from the cylinder, $r \gg R$, equation (21) provides

$$\phi_n(r, \theta) \sim \tilde{\phi}_n(\theta) \frac{e^{ikr}}{\sqrt{r}},$$

$$\tilde{\phi}_n(\theta) = \sqrt{\frac{2}{\pi k}} e^{-i\frac{\pi}{4}} \left( \frac{1}{2} \frac{G_{n0}^{(c)}}{kH_0^{(1)'}(kR)} + \sum_{m=1}^{\infty} [G_{nm}^{(c)} \cos(m\theta) + G_{nm}^{(s)} \sin(m\theta)] \frac{(-i)^m}{kH_m^{(1)'}(kR)} \right). \tag{27}$$

The functions $\tilde{\phi}_n(\theta)$, $n \geq 1$, depend on the Fourier coefficients $f_m^{(c)}$, $f_m^{(s)}$, $m \geq 0$, of the function $f(\theta)$. This dependence is linear for $\tilde{\phi}_1(\theta)$ and quadratic for $\tilde{\phi}_2(\theta)$. The obtained asymptotic formula for the diffracted wave field can be used to determine the shape of a vertical cylinder by using the wave measurements far from it.

Let us assume that we know the incident wave and the diffracted wave field (elevation of the water surface) far from a cylinder. Let us assume that the cylinder is vertical but we do not know the shape of its cross section and the position of the cylinder. By analyzing the measured diffracted wave field and the derived first order approximation of the potential

$$\phi(r,\theta) \sim [\tilde{\phi}_0(\theta) + \varepsilon\tilde{\phi}_1(\theta)]\frac{e^{ikr}}{\sqrt{r}} \quad (r \to \infty), \tag{28}$$

we can estimate the radius of the cylinder $R$, position of its center, the scale of its surface perturbation $\varepsilon$, and the Fourier coefficients $f_m^{(c)}$ and $f_m^{(s)}$ of the deviation, $f(\theta)$, of the cylinder cross section from the circular one. This problem of the cylinder identification is not considered in this paper. The algorithm of this study relates the function $\tilde{\phi}_1(\theta)$ and the shape function $f(\theta)$, which is crucial for efficient solution of the identification problem.

In some problems, the shape function can also depend on the small parameter $\varepsilon$, $r = R[1 + \varepsilon f(\theta, \varepsilon)]$, and can be approximated as

$$f(\theta,\varepsilon) = f_0(\theta) + \varepsilon f_1(\theta) + \varepsilon^2 f_2(\theta) + \varepsilon^3 f_3(\theta) + \varepsilon^4 f_4(\theta) + \mathcal{O}(\varepsilon^5). \tag{29}$$

The asymptotic expansion (29), where each function $f_n(\theta)$ is presented by its Fourier series, is substituted in (16) and we again arrive at the boundary conditions in the form (19) but with different functions $G_n(\theta)$. In particular, $f(\theta)$ is changed to $f_0(\theta)$ in (18). The expansion (29) will be used in the next section to find approximate solution of the problem for an elliptic cylinder of a small eccentricity.

## HYDRODYNAMIC FORCE ON ELLIPTIC VERTICAL CYLINDER

To validate the algorithm of the present paper, which is based on the asymptotic formula and operations with the Fourier coefficients, the algorithm is applied to the problem of elliptic vertical cylinders. This problem has been solved by Chen and Mei (1971) by series of the Mathieu functions and elliptic coordinates, and by Williams (1985) using the method of integral equation on the boundary of the cylinder. Williams (1985) also used the asymptotic behaviors of the Mathieu functions to derive asymptotic formula for the total force components when the eccentricity of the elliptic section is small.

In this section, the vertical cylinder with elliptic cross section of small eccentricity $e = \sqrt{1 - b^2/a^2}$, where $a$ is the semi-major axis and $b$ is the semi-minor axis of the elliptic cross section is considered. The equation of the ellipse in the polar coordinates $r$, $\theta$ with the origin at the focus of the ellipse reads

$$r = \frac{a(1-e^2)}{1 - e\cos\theta}\,. \tag{30}$$

Taking the eccentricity $e$ as a small parameter of the problem, $\varepsilon = e$, and calculating the Fourier coefficients of the right-hand side in (30), we obtain

$$\begin{aligned} r &= a\sqrt{1-\varepsilon^2} + 2a\sqrt{1-\varepsilon^2}\sum_{n=1}^{\infty}\left[\frac{\varepsilon}{1+\sqrt{1-\varepsilon^2}}\right]^n \cos(n\theta) \\ &= a + \varepsilon a\cos\theta + \varepsilon^2 a\left(\tfrac{-1+\cos(2\theta)}{2}\right) + \varepsilon^3 a\left(\tfrac{-\cos\theta+\cos(3\theta)}{4}\right) + \varepsilon^4 a\left(\tfrac{-1+\cos(4\theta)}{8}\right) + \mathcal{O}(\varepsilon^5). \end{aligned} \tag{31}$$

Comparing (31) with the equation of the cylinder in the present analysis, $r = R[1+\varepsilon f(\theta,\varepsilon)]$, and expansion (29), we find

$$R = a,\ f_0(\theta) = \cos\theta,\ f_1(\theta) = -\frac{1}{2} + \frac{1}{2}\cos(2\theta),$$

$$f_2(\theta) = -\frac{1}{4}\cos\theta + \frac{1}{4}\cos(3\theta),\ f_3(\theta) = -\frac{1}{8} + \frac{1}{8}\cos(4\theta).$$

The non-dimensional force components $\tilde{F}_x$ and $\tilde{F}_y$ are calculated by the present algorithm using equation (26), equation (12) for the potential $\phi_0(R,\theta)$ on the cylinder at leading order and equations (21) for the higher order potentials $\phi_n(R,\theta)$, where $n = 1,2,3,4$. The modulus of the force components $|\tilde{F}_x|$ and $|\tilde{F}_y|$ are calculated by the fifth-order approximation (15) and also by the third-order approximation keeping only three terms in (15). The forces are calculated for $0 < ka < 4$ and the eccentricity $e = 1/2$. The obtained forces are compared with the results by Williams (1985) in Figures 2(a) and 2(b).

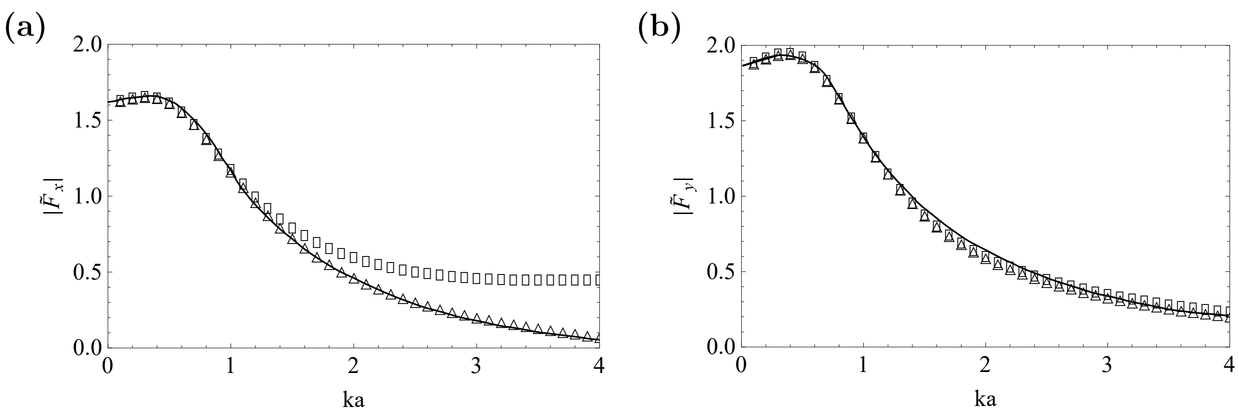


FIG. 2: The $x$ and $y$-components of the non-dimensional force acting on elliptic cylinder for $e = 0.5$, $\alpha = 0°$ in (a) and $\alpha = 90°$ in (b). The solution by Williams (1985) is shown by solid line, and the present asymptotic solutions are shown by markers: □ is for the third-order and △ is for the fifth-order asymptotic solutions.

It was found for this range of $ka$ that the five terms in (12) and (21) provide accurate results. At the end of each operation with the Fourier series, the resulting series was truncated to five terms with cosines and five terms with sines. Note that the forces were computed by Williams (1985) by two different methods depending on the value of the product $ka$. For large $ka$ the forces were computed by the boundary element method, and for small $ka$ the solution was found in the series form involving Mathieu functions. In the boundary element method, the elliptic contour was divided into 120 elements. Due to problems with convergence of the series of the Mathieu functions, Williams (1985) used the asymptotic formula of these functions for small eccentricity $e$ and obtained fifth-order approximations of the force components up to $\mathcal{O}(e^5)$ terms. The formula for the coefficients in the asymptotic formula by Williams (1985) are collected in four-page appendix at the end of his paper. The approach of the present paper is more straightforward and provides the approximations of the force components of the same order as by Williams (1985) for small eccentricity. The Mathieu functions in the infinite series solution depend on the parameter $q = (kae)^2/4$. Williams (1985) suggested to use his asymptotic formula for $q \leqslant 0.4$ and the boundary element method for $q > 0.4$. This implies that, in Figures 2(a) and 2(b), the solid lines representing the forces by Williams (1985) for $e = 1/2$ were computed by his asymptotic formula for $0 < ka < 2.5$. The Figures 2(a) and 2(b) show that our asymptotic fifth-order solutions is very close to the forces computed by Williams (1985). The present asymptotic solution in the long-wave approximation, $ka \to 0$, provides

$$\tilde{\mathcal{F}}_x(t) = \left[2 - \frac{3}{2}\varepsilon^2 - \frac{1}{8}\varepsilon^4 + \mathcal{O}(\varepsilon^6)\right]\cos(\omega t), \tag{32}$$

for $\alpha = 0°$ and

$$\tilde{\mathcal{F}}_y(t) = \left[2 - \frac{1}{2}\varepsilon^2 - \frac{1}{8}\varepsilon^4 + \mathcal{O}(\varepsilon^6)\right]\cos(\omega t), \tag{33}$$

for $\alpha = 90°$. The asymptotic formula (32) and (33) coincide with those derived by Williams (1985).

## HYDRODYNAMIC FORCE ON SQUARE VERTICAL CYLINDER

Let equation $r = a\,F(\theta)$ describe the square, $x = \pm a,\ -a < y < a$ and $y = \pm a,\ -a < x < a$, in the polar coordinates, $x = r\cos\theta$ and $y = r\sin\theta$. We shall determine the Fourier coefficients of the function $F(\theta),\ 0 \leqslant \theta \leqslant 2\pi$, and then convert the corresponding Fourier series into the form $r = R[1 + \varepsilon f(\theta)]$ identifying values of $R,\ \varepsilon$ and the function $f(\theta)$. Then the approach of the section "Vertical Cylinders with Nearly Circular Cross Sections" will give the components of the total hydrodynamic force acting on the square cylinder.

A square has four lines of symmetry, $F(-\theta) = F(\theta),\ F\left(\frac{\pi}{2} - \theta\right) = F\left(\frac{\pi}{2} + \theta\right),\ F\left(\frac{\pi}{4} - \theta\right) = F\left(\frac{\pi}{4} + \theta\right)$. The Fourier series of the function $F(\theta)$ contains only $\cos(4m\theta),\ m \geqslant 0$;

$$F(\theta) = \frac{1}{2}F_0 + \sum_{m=1}^{\infty} F_m \cos(4m\theta),$$

$$F_m = \frac{8}{\pi}\int_0^{\pi/4} F(\theta)\cos(4m\theta)\,\mathrm{d}\theta = \frac{8}{\pi}\int_0^{\pi/4} \frac{\cos(4m\theta)}{\cos\theta}\,\mathrm{d}\theta,$$

where $F_0 = \dfrac{8}{\pi}\log(1+\sqrt{2})$ and $F_m = \dfrac{16}{\pi}\sqrt{2}(-1)^m/[(4m-1)(4m-3)] + F_{m-1},\ m \geqslant 1$. Therefore

$$R = a\,F_0/2 \approx 1.1222a.$$

The maximum value of $F(\theta)$ is $\sqrt{2}$, which gives $\varepsilon = 2\sqrt{2}/F_0 - 1 \approx 0.26$ and $|f(\theta)| \leqslant 1$, where

$$f(\theta) = \sum_{m=1}^{\infty} f_m \cos(4m\theta), \quad f_m = 2F_m/(\varepsilon F_0), \tag{34}$$

$f_1 = -0.5357,\ f_2 = 0.1689,\ f_3 = -0.0801,\ f_4 = 0.0463,\ f_5 = -0.03$. The shapes given by the equation $r = R[1 + \varepsilon f(\theta)]$ with three terms (dashed line) and ten terms (solid line)

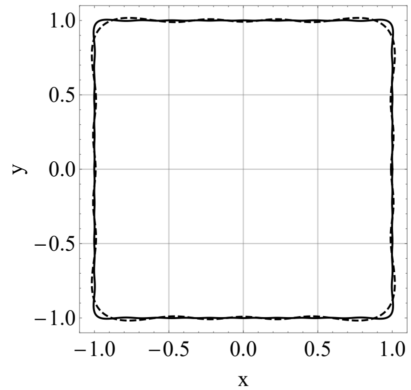


FIG. 3: The approximation of the square by the equation $r = R[1 + \varepsilon f(\theta)]$ in the polar coordinates with three (dashed line) and ten (solid line) terms retained in the series (34).

retained in the series (34) are shown in Figure 3. It is seen that the approximation of the square cross section with only three terms in the series (34) is reasonably good.

Hydrodynamic forces acting on a square caisson have been studied by Mogridge and Jamieson (1976). They performed experiments with a 30.48cm $\times$ 30.48cm (12in $\times$ 12in) square box in the wave flume 3.65m (12ft) wide, 1.37m (4.5ft) deep and 49.3m (162ft) long. The hydrodynamic forces for $\alpha = 0°$ were measured and compared with the predictions by the theory of "equivalent circular radius". In this theory of equivalent circular radius, the horizontal hydrodynamic force on a vertical cylinder with the area of its cross section $|D|$ is approximated by the force acting on the circular cylinder of radius $R_e$, where the area of the circular cross section, $\pi {R_e}^2$, is equal to the area $|D|$. For the square shape vertical cylinder with $|D| = (2a)^2$, we obtain $R_e = 2a/\sqrt{\pi} \approx 1.1283a$. It is seen that the "equivalent radius" $R_e$ is very close to the radius $R \approx 1.1222a$ calculated above by using the Fourier series.

The computed hydrodynamic forces acting on the square vertical cylinder with $\alpha = 0°$ are shown in Figure 4. The fifth-order approximation (15) was used. Note that $\varepsilon^5 < 0.0012$. Representing the square with four terms in (34) and truncating the Fourier series of the potentials $\phi_n$, $n = 0, 1, 2, 3, 4$, in (21) to sixteen terms, the force shown by the dashed line is obtained. The computed force is very close to the experimental results by Mogridge and Jamieson (1976) which are shown by markers. Keeping just one term in (34) and four terms in the Fourier series (21), we arrive at the solid line which is very close to the prediction of the force with four terms in (34), where $1 \leqslant ka \leqslant 4$, but underpredicts the force in the interval $0 \leqslant ka \leqslant 1$. The force predicted by the "equivalent circular radius" theory of Mogridge and Jamieson (1976) is shown by the dotted line in Figure 4. This prediction of the force is very close to our asymptotic force with one term in (34), where $0 \leqslant ka < 2$. We conclude that more terms in (34) provide better approximation of the experimental force for long waves but do not improve the prediction of the hydrodynamic force for short waves.

## HYDRODYNAMIC FORCE ON QUASI-ELLIPTIC VERTICAL CYLINDER

A quasi-ellipse consists of a rectangular part in the center and two semicircular parts at the front and back (see Figure 5(a)). In Figure 5(a), $D/2$ is the radius of the semicircles and $B$ is the length of the rectangular part.

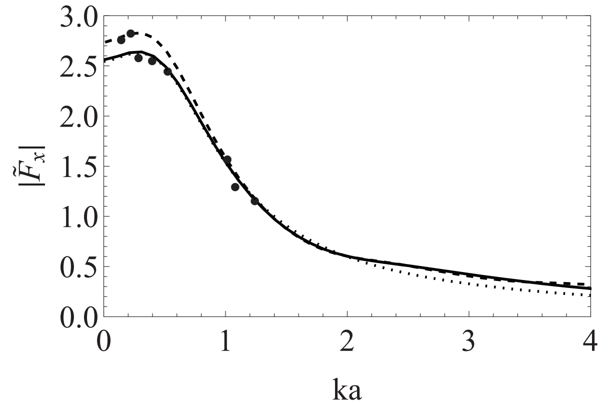


FIG. 4: The non-dimensional hydrodynamic force acting on the square vertical cylinder in waves. Comparison of Mogridge and Jamieson theory (dotted line), experimental results (• markers), the present method with one term in (34) (solid line) and present method with four terms in (34) (dashed line).

Let equation $r = F(\theta)$ describe the quasi-ellipse in Figure 5(a) in the polar coordinates, $x = r\cos\theta$ and $y = r\sin\theta$, where

$$F(\theta) = \begin{cases} \dfrac{B\cos\theta + \sqrt{D^2 - B^2\sin^2\theta}}{2}, & 0 \le \theta \le \arctan\dfrac{D}{B}, \\ \dfrac{D}{2\sin\theta}, & \arctan\dfrac{D}{B} \le \theta \le \pi - \arctan\dfrac{D}{B}, \\ \dfrac{-B\cos\theta + \sqrt{D^2 - B^2\sin^2\theta}}{2}, & \pi - \arctan\dfrac{D}{B} \le \theta \le \pi + \arctan\dfrac{D}{B}, \\ \dfrac{-D}{2\sin\theta}, & \pi + \arctan\dfrac{D}{B} \le \theta \le 2\pi - \arctan\dfrac{D}{B}, \\ \dfrac{B\cos\theta + \sqrt{D^2 - B^2\sin^2\theta}}{2}, & 2\pi - \arctan\dfrac{D}{B} \le \theta \le 2\pi. \end{cases}$$

We shall determine the Fourier coefficients of the function $F(\theta),\ 0 \leqslant \theta \leqslant 2\pi$, and then convert the corresponding Fourier series into the form $r = R[1 + \varepsilon f(\theta)]$ identifying values of $R,\ \varepsilon$ and the function $f(\theta)$. Then the approach of the section "Vertical Cylinders with Nearly Circular Cross Sections" will give the components of the total hydrodynamic force acting on the quasi-elliptic cylinder.

A quasi-ellipse has two lines of symmetry, $F(-\theta) = F(\theta),\ F\left(\frac{\pi}{2} - \theta\right) = F\left(\frac{\pi}{2} + \theta\right)$. Hence, the Fourier series of the function $F(\theta)$ contains only $\cos(2m\theta),\ m \geqslant 0$;

$$F(\theta) = \frac{1}{2}F_0 + \sum_{m=1}^{\infty} F_m \cos(2m\theta),$$

$$F_m = \frac{1}{\pi}\int_0^{2\pi} F(\theta)\cos(2m\theta)\,\mathrm{d}\theta = \frac{4}{\pi}\int_0^{\pi/2} F(\theta)\cos(2m\theta)\,\mathrm{d}\theta, \quad m = 0, 1, 2, \cdots.$$

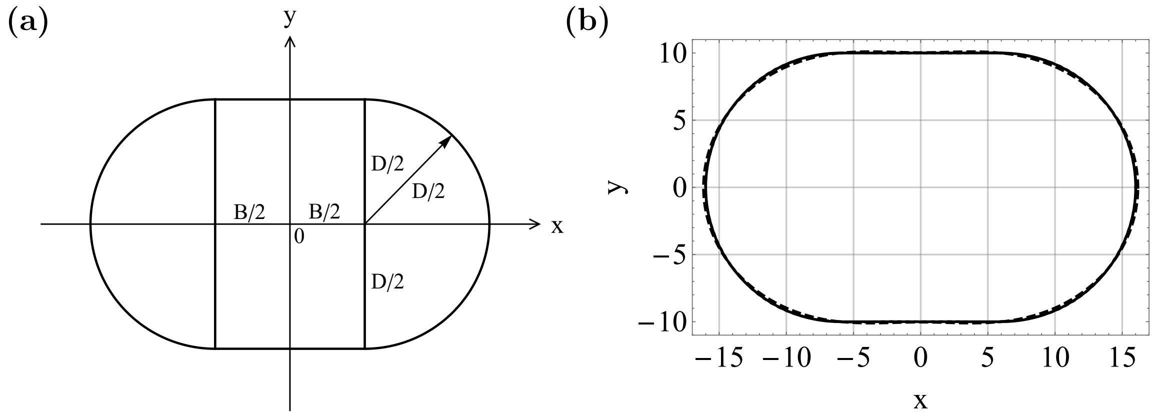


FIG. 5: (a) Quasi-ellipse. (b) The approximation of the quasi-ellipse by the equation $r = R[1 + \varepsilon f(\theta)]$ in the polar coordinates with two (dashed line) and eight (dotted line) terms retained in the series (35) and the exact shape of quasi-ellipse (solid line).

The Fourier coefficients $F_m$, $m = 0, 1, 2, \ldots$, are evaluated for $D = 20$ m and $B = 12$ m. These particular values were used by Wang et al. (2011). Then,

$$R = F_0/2 \approx 13.1026\,\mathrm{m}.$$

The maximum value of $F(\theta)$ is $(D + B)/2$, which gives $\varepsilon = (B + D)/F_0 - 1 \approx 0.221136$ and $|f(\theta)| \leqslant 1$, where

$$f(\theta) = \sum_{m=1}^{\infty} f_m \cos(2m\theta), \quad f_m = 2F_m/(\varepsilon F_0), \tag{35}$$

$f_1 = 3.06712$, $f_2 = -0.145175$, $f_3 = -0.0595601$, $f_4 = 0.050526$, $f_5 = -0.0148836$, $f_6 = -0.00652338$, $f_7 = 0.00973661$. The shapes given by the equation $r = R[1 + \varepsilon f(\theta)]$ with two terms (dashed line) and eight terms (solid line) retained in the series (35) are shown in Figure 5(b). It is seen that the approximation to the quasi-elliptic cross section with eight terms in the series (35) is reasonably good.

Wang et al. (2011) developed a three dimensional time domain method to solve the Navier Stokes equations including viscosity and nonlinear effects. Wave forces on the quasi-ellipse caisson are calculated and compared with the results of Wang et al. (2011) (see Figure 6). For comparison purposes, the vertical axis in the Figure 6 is chosen as $F_x^* = [\pi ka/4]\widetilde{F}_x$, $a = (B + D)/2 = 0.8D$. It is seen from the Figure 6 that there is small discrepancy between the present results and the results of Wang et al. (2011), which can be attributed to the effect of viscosity and nonlinearity considered in the Navier Stokes formulation of Wang et al. (2011). Figure 6 shows that the present approach gives slightly smaller values for wave forces compared with the Navier Stokes computations. However, the present model still can be used to make a quick study to identify critical wave numbers and directions as input to more detailed and computationally more expensive Navier Stokes computations.

For the incident wave propagating at an angle $\alpha$ to the positive $x$-axis, the wave force and the maximum wave runup are computed and compared for cylinders of circular, elliptic, quasi-elliptic and square cross sections, see Figure 7, with the same cross sectional area. The

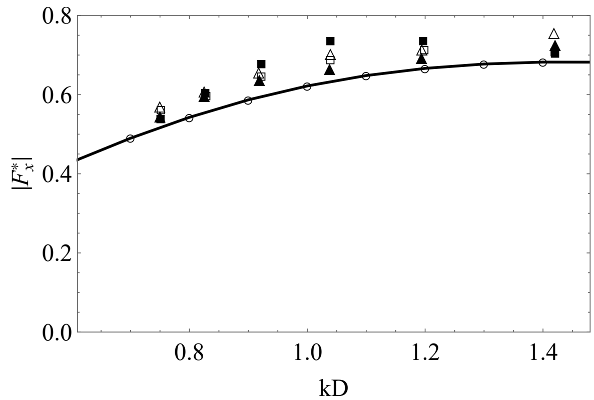


FIG. 6: The non-dimensional hydrodynamic force acting on the quasi-elliptic vertical cylinder in waves. Wang ($H/h = 0.05$, ■ markers), Wang ($H/h = 0.095$, □ markers), Wang ($H/h = 0.15$, ▲ markers), Wang ($H/h = 0.2$, △ markers), the present method with fourteen terms in (35), (line with ∘ markers). Here $H$ is the wave height, $H = 2A$, and $h$ is the water depth.

forces and maximum runups for $\alpha = 0°$ are compared in Figures 8(a) and 8(b), respectively. It is observed from Figure 8(a) that wave force is smallest for the cylinder with quasi-elliptic cross section, and from Figure 8(b) that maximum non-dimensional wave runup is highest for the square cylinder. For the incident wave propagating at angle $\alpha = 90°$ to the positive $x$-axis, see Figure 7, wave forces for elliptic and quasi-elliptic cylinders are higher than for $\alpha = 0°$. This can be attributed to the larger projected area normal to the flow of these cylinders for $\alpha = 90°$. The computations for $\alpha = 90°$ provide that the wave force is highest for the cylinder with quasi-elliptic cross section and the maximum non-dimensional wave runup is highest for quasi-elliptic cylinder, where $0 < ka < 1.1$, and for square cylinder, where $1.1 < ka < 4$. Figures for the latter case is not included. It is concluded that the forces are dependent on angle of wave incidence, $\alpha$, with the corresponding corrections of order $O(\varepsilon)$, see equation (26), where $S_{00}^{(c)}$ is independent of $\alpha$.

## HYDRODYNAMIC FORCE AND WAVE RUNUP ON THE CYLINDER WITH COSINE TYPE RADIAL PERTURBATIONS

Vertical cylinders with cosine type radial perturbations of their cross section,

$$r = R[1 + \varepsilon \cos(N\theta)], \tag{36}$$

where $N$ is a positive integer, were studied by Mansour et al. (2002). The cross sections of the cylinders in equation (36) are shown in Figure 9 for $R = 1$ m, $\varepsilon = 0.05$ and $N = 1, 2, 3, 4, 5, 6$.

Mansour et al. (2002) derived the leading order corrections to the forces acting on the cylinders (36) as $\varepsilon \to 0$, and also to the maximum non-dimensional runup, $\triangle_{max}/2A$, for these cylinders. They also computed the hydrodynamic forces and wave runups by the method of boundary integral equation and compared their numerical and first-order asymptotic results. They concluded that the first-order asymptotic solutions well agree with the numerical solutions in the range $0 \leq \varepsilon \leq 0.05$. The higher-order asymptotic solution of the

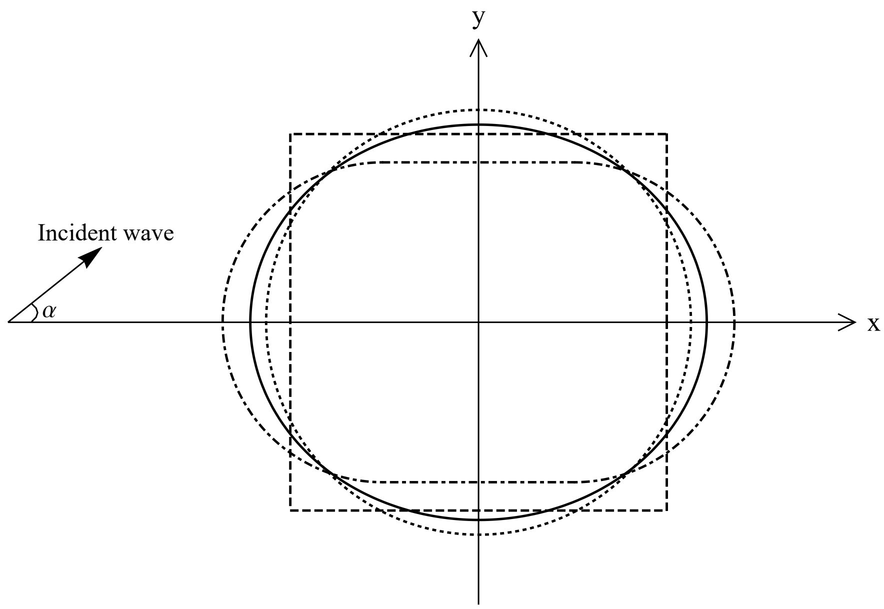


FIG. 7: Orientation of quasi-elliptic (dotdashed line), elliptic (solid line), square (dashed line) and circular (dotted line) cylinders relative to incident wave.

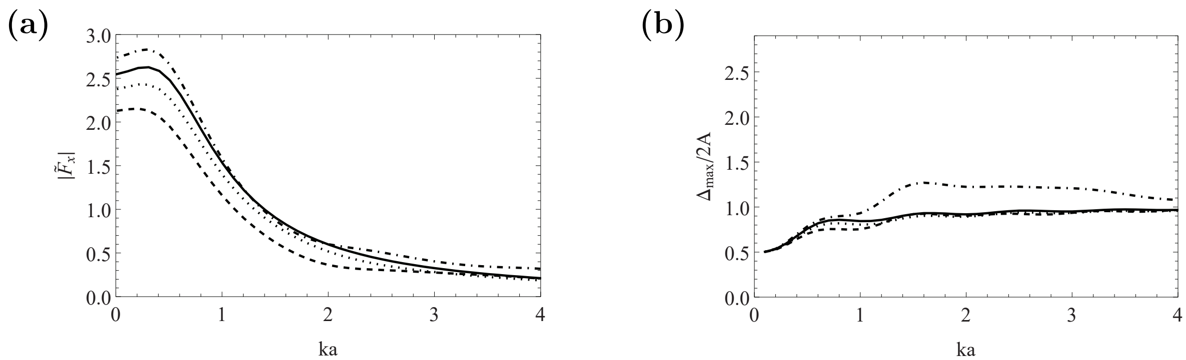


FIG. 8: (a) The non-dimensional hydrodynamic force and (b) the maximum non-dimensional wave runup on cylinders of circular (solid line), elliptical (dotted line), quasi-elliptical (dashed line) and square (dotdashed line) cross sections with same cross sectional areas. Angle of wave incidence, $\alpha$, is zero.

present paper provides the forces and runups almost identical with the numerical forces and runups by Mansour et al. (2002), see Figures 10 and 11. It is observed that the present approach compares quite well with the integral equation method of Mansour et al. (2002) even for high values of $kR$. Note that the asymptotic results by Mansour et al. (2002) for the maximum non-dimensional wave runup deviate significantly from their numerical results for $kR \geq 1$.

To compare the forces computed by Mansour et al. (2002) with the results of the present method, the forces in (7) and (8) are multiplied by $(1/2)\tanh(kh)$. The resulting non-

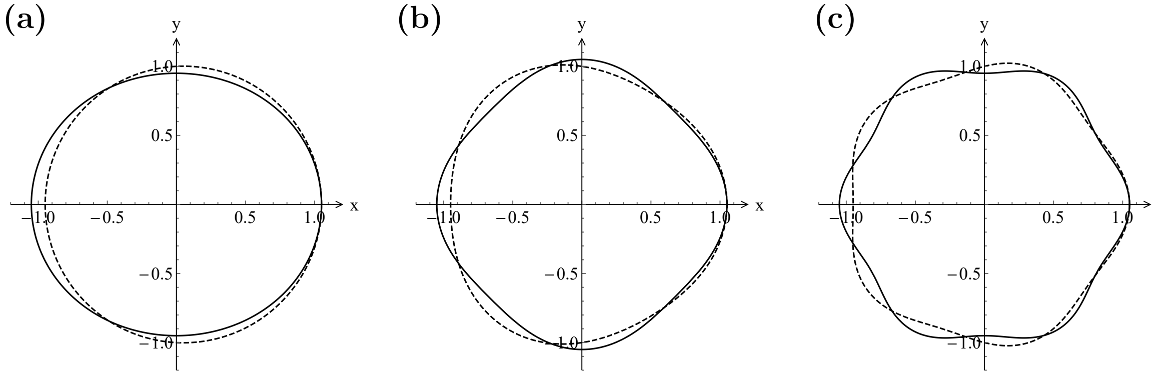


FIG. 9: The cross sections of the cylinders (36) for $R = 1$ m, $\varepsilon = 0.05$ and (a) $N = 1$ (dashed line), $N = 2$ (solid line), (b) $N = 3$ (dashed line), $N = 4$ (solid line), (c) $N = 5$ (dashed line), $N = 6$ (solid line).

dimensional forces $|\overline{F}_x| = [(1/2)\tanh(kh)]|\widetilde{F}_x|$ are shown in Figures 10(a1-a4) for $N = 2, 3, 4$ and 6 in (36). These figures demonstrate that the first-order asymptotic forces by Mansour et al. (2002) are very close to both the numerical results and to our higher-order forces for $\varepsilon = 0.05$ and $0 < kR < 4$. The maximum runup $\triangle_{max}/(2A)$ is more sensitive to the number of terms in the asymptotic solution (15), see Figures (10)(b1-b4). It is seen that our fifth-order asymptotic solution provides the wave runup almost identical with the numerical solution for $\varepsilon = 0.05$. This conclusion is also true for $\varepsilon = 0.1$, see Figure 11, for both the force and the maximum runup as functions of the non-dimensional wave number, $kR$. Note that the first-order asymptotic solution cannot be used for $\varepsilon = 0.1$.

The present method is restricted to vertical cylinders whose cross sections are close to a circle. Liu et al. (2016) solved numerically the problem (2) - (4) with no restriction on the shape of the cylinder cross section. The method they use is not an asymptotic method but a Fourier series method combined with the Galerkin method to satisfy the body condition (4). However, authors reported some difficulties with the system of equations they obtained. The system is ill posed for some cases after truncating the infinite system of equations. Despite the reported difficulties, their results show good agreement with numerical results by Mansour et al. (2002). In the present method we deal only with multiplication and summation of Fourier series to find the unknown potentials $\phi_n$, $n = 1, 2, 3, 4$, so the present method is stable in solving the wave diffraction problem for vertical cylinders.

The effect of the truncation of the Fourier series (12), (21) and (22) on the performance of the present asymptotic solution is demonstrated by Figures 12 and 13. Let the number of terms $m$ vary from 1 to $p$ in (21) and (22). After each multiplication of two Fourier series the resulting Fourier series is truncated to $p$ terms. The system of the equation in the method of Liu et al. (2016) is truncated in a similar way because Fourier series are used to represent the body shape and the velocity potential.

Liu et al. (2016) recommended $p = 20$ for any shapes of the cylinders with cosine type section. It was observed that $p = 12$ in our asymptotic solution provides good agreement with the numerical results by Liu et al. (2016). Even $p = 6$ in our method provides a very reasonable agreement with the numerical force and maximum runup. The distributions of the wave runup along the cylinder are shown in Figure 13 for $p = 20$ in the computations

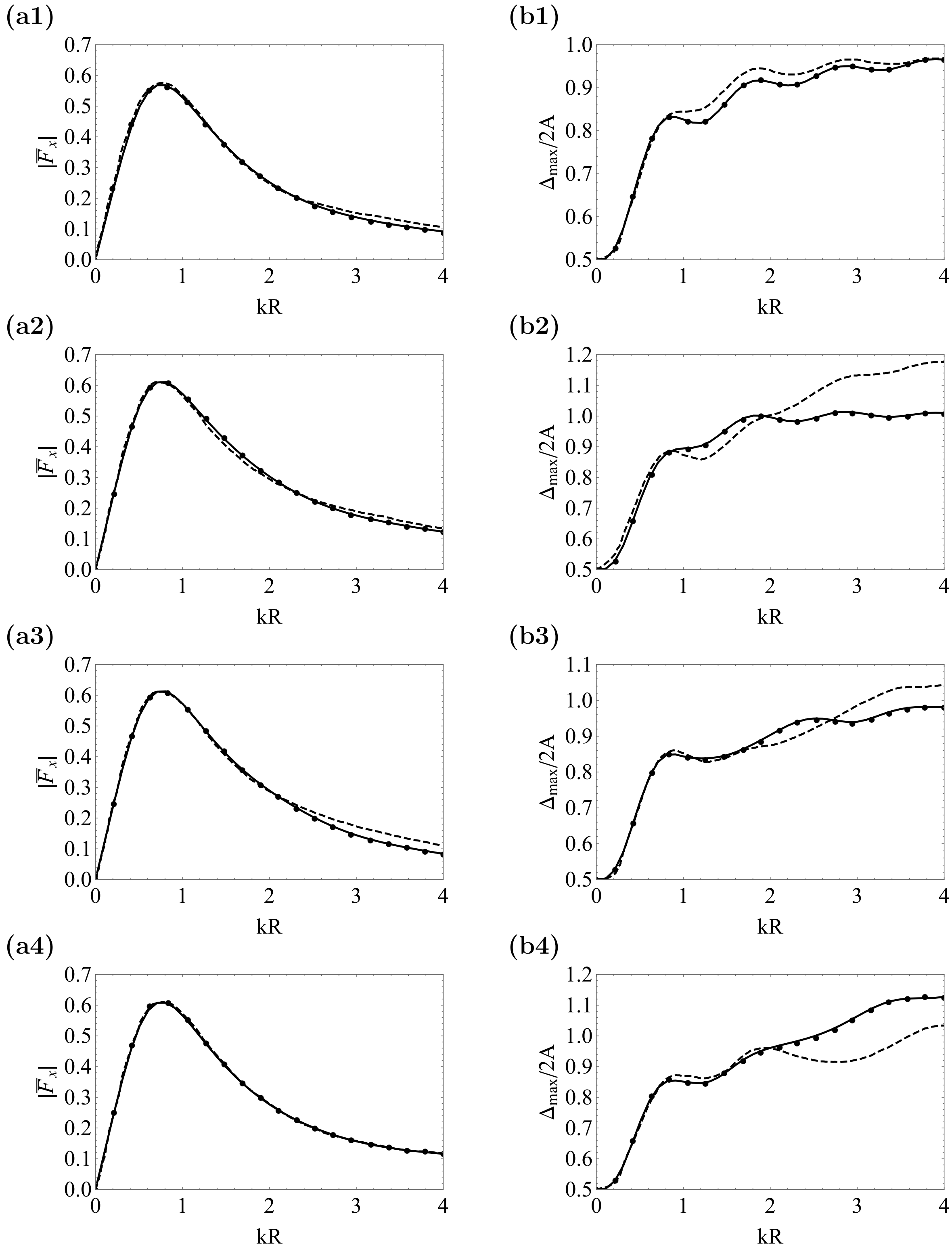


FIG. 10: (a1)-(a4) The non-dimensional hydrodynamic force and (b1)-(b4) the maximum non-dimensional wave runup on the vertical cylinder in (36). Comparison of the results by the present method (solid line) with the analytical (dashed line) and numerical (• markers) results by Mansour et al. (2002) for $\varepsilon = 0.05$ and $N = 2$ in (a1), (b1), $N = 3$ in (a2), (b2), $N = 4$ in (a3), (b3) and $N = 6$ in (a4), (b4).

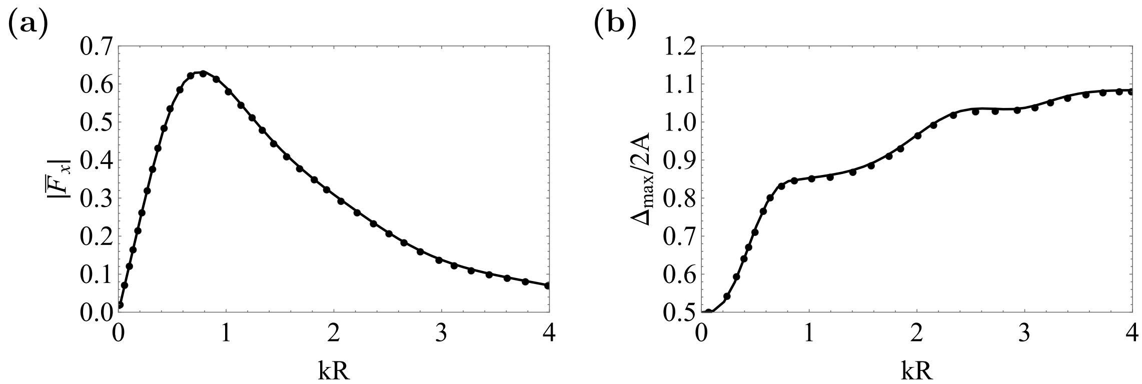


FIG. 11: (a) The non-dimensional hydrodynamic force and (b) the maximum non-dimensional wave runup on the vertical cylinder in (36). Comparison of the present method (solid line) with Mansour et al. (2002)'s numerical method (• markers) for $\varepsilon = 0.1$ and $N = 4$.

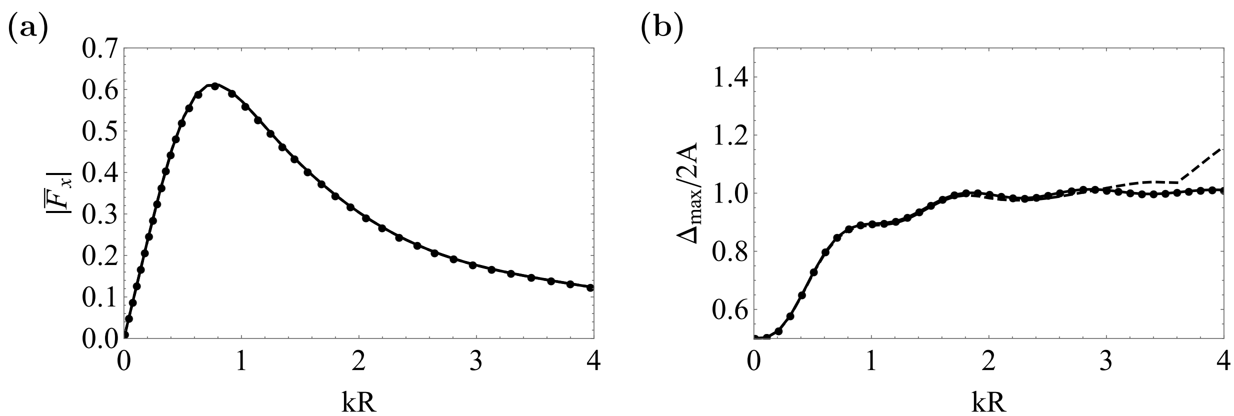


FIG. 12: The effect of the truncation number $p$ on the non-dimensional (a) hydrodynamic force and (b) maximum wave runup for $\varepsilon = 0.05$, $N = 3$ in (36). Liu et al. (2016) numerical method with $p = 9$, 20 (• markers), the present method with $p = 4$ (dashed line), $p = 9$ (solid line).

by Liu et al. (2016) and $p = 6, 12$ in our calculations. It is seen that the predictions of the wave runup by the present method are good even for waves with $kR = 4$.

## LONG WAVE APPROXIMATION OF WAVE FORCES

The formula (5) for the hydrodynamic force $\mathbf{F}(t)$ acting on a vertical cylinder with cross section $D$ can be simplified for long waves, where $ka \to 0$ and $a$ is a characteristic dimension of the cylinder cross section. We shall use the ideas by Haskind (1973, Chapter 2), who expressed the forces as integrals of the potential of the incident wave, three radiation potentials and their normal derivatives on the cylinder. The radiation potentials describe waves generated by the cylinder oscillating in $x-$ and $y-$directions and due to torsional oscillation of the cylinder. Haskind also introduced generalized added masses and damping coefficients of vertical cylinders as functions of the non-dimensional wave number $ka$. The

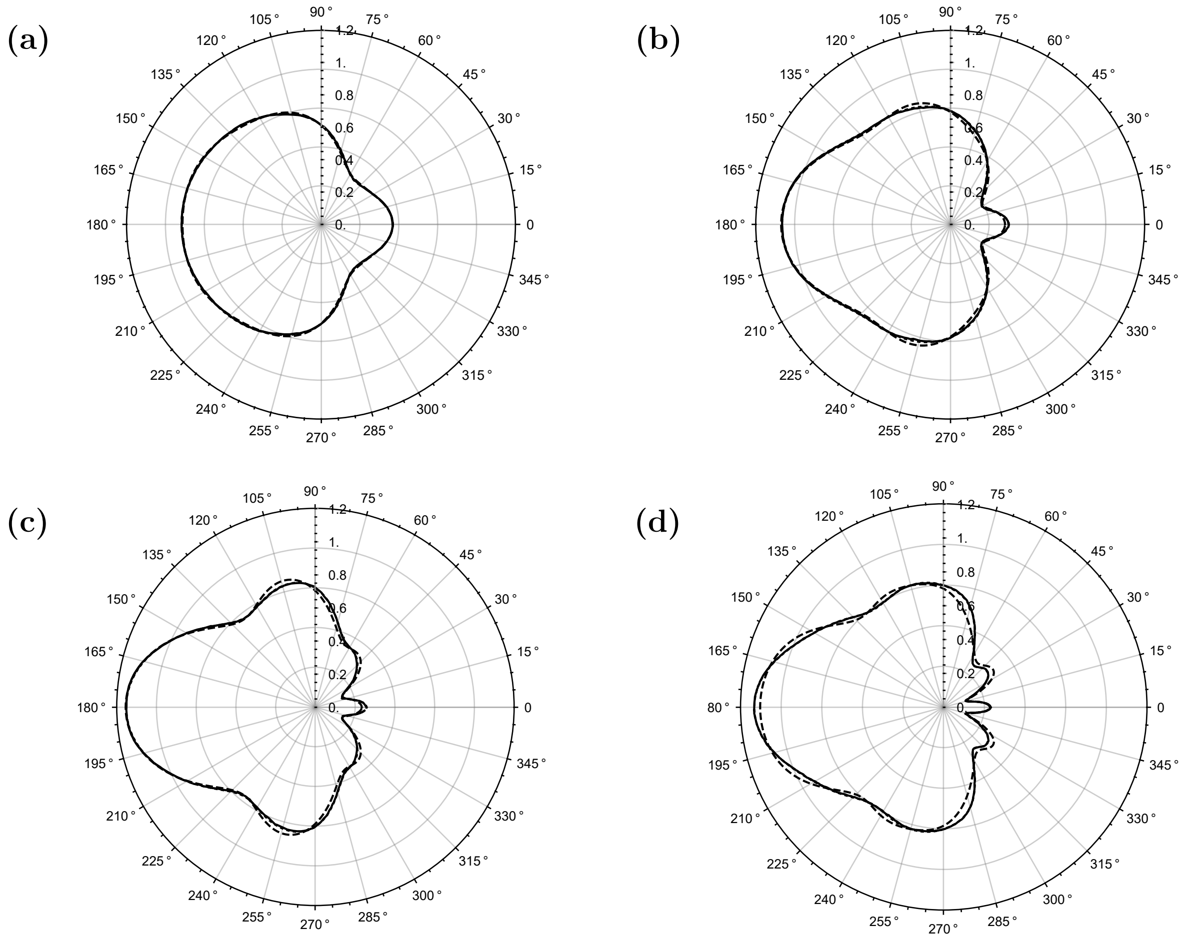


FIG. 13: The non-dimensional wave runup, $\triangle(\theta)/2A$, for the cylinder (36) with $\varepsilon = 0.05$ and $N = 5$ computed for (a) $kR = 1$, (b) $kR = 2$, (c) $kR = 3$, (d) $kR = 4$. The present asymptotic method with $p = 6$ (dashed line) and $p = 12$ (dotted line) is compared with the numerical results (solid line) by Liu et al. (2016) with $p = 20$.

generalized added masses approach the added masses of the two-dimensional body $D$ moving in unbounded incompressible liquid as $ka \to 0$. In this section, we limit ourselves to the force component only in the direction of the incident wave propagation in the limit as $ka \to 0$, with $\alpha = 0°$.

Equations (5) and (6) provide the non-dimensional $x-$component of the hydrodynamic force acting on the cylinder,

$$\tilde{F}_x = \frac{-i}{\pi a^2 k} \int_{\partial D} \phi(r,\theta)\, n_x \, \mathrm{d}s, \tag{37}$$

where $\phi(r,\theta)$ is the solution of the problem (2)-(4) and $n_x$ is the $x-$component of the unit normal vector $\mathbf{n}$ to the surface of the cylinder. It is convenient to introduce new potential $\varphi(x,y)$ by the equation $\phi(r,\theta) = e^{ikx} - ik\,\varphi(x,y)$. The potential $\varphi(x,y)$ satisfies equation (2), describes outgoing waves as $r \to \infty$, and its normal derivative on the cylinder is given by

$$\frac{\partial \varphi}{\partial n} = e^{ikx} n_x \quad (\text{on } \partial D). \tag{38}$$

By using the potential $\varphi(x, y)$ and condition (38), the force (37) can be presented in the form

$$\tilde{F}_x = \frac{1}{\pi a^2} \left\{ -\frac{i}{k} \int_{\partial D} e^{ikx}\, n_x \, \mathrm{d}s - \int_{\partial D} \varphi \, \frac{\partial \varphi}{\partial n} \, e^{-ikx} \, \mathrm{d}s \right\}. \tag{39}$$

The product $e^{ikx}\, n_x$ in the first integral of (39) can be viewed as the scalar product of two vectors: $(e^{ikx}, 0)$ and $\mathbf{n}$. Then the divergence theorem yields

$$-\frac{i}{k} \int_{\partial D} e^{ikx}\, n_x \, \mathrm{d}s = -\frac{i}{k} \int_D div(e^{ikx}, 0) \, \mathrm{d}x\mathrm{d}y = \int_D e^{ikx} \, \mathrm{d}x\mathrm{d}y.$$

Taking the limit in (39) as $ka \to 0$, where $x/a = \mathcal{O}(1)$, we obtain

$$\tilde{F}_x(0) = \frac{1}{\pi a^2} \left[ |D| - \int_{\partial D} \varphi_0 \, \frac{\partial \varphi_0}{\partial n} \, \mathrm{d}s \right], \tag{40}$$

where $|D|$ is the area of the cylinder cross section and $\varphi_0(x, y)$ is the limiting value of the potential $\varphi(x, y)$ as $ka \to 0$. The potential $\varphi_0(x, y)$ satisfies the following equations

$$\begin{aligned} \nabla^2 \varphi_0 &= 0 \quad (\text{outside } D), \\ \frac{\partial \varphi_0}{\partial n} &= n_x \quad (\text{on } \partial D), \\ \varphi &\to 0 \quad (x^2 + y^2 \to \infty), \end{aligned}$$

and describes the two-dimensional flow caused by the motion of the body $D$ in unbounded and incompressible liquid in the $x-$direction at the unit speed. The integral in (40) multiplied by $-\rho$ is known as the added mass $m_{xx}$. Finally

$$\tilde{F}_x(0) = \frac{1}{\pi a^2} \left[ |D| + \frac{m_{xx}}{\rho} \right]. \tag{41}$$

For the elliptic cylinder $x^2/a^2 + y^2/b^2 = 1$ with the semi-major axis $a$ and the semi-minor axis $b$, where $b = a\sqrt{1 - e^2}$ and $e$ is the eccentricity of the ellipse, we have $|D| = \pi ab$, $m_{xx} = \rho \pi b^2$ and (41) gives

$$\tilde{F}_x(0) = \frac{b}{a} + \frac{b^2}{a^2} = \sqrt{1 - e^2} + 1 - e^2 = 2 - \frac{3}{2}e^2 - \frac{1}{8}e^4 + \mathcal{O}(e^6),$$

which corresponds to the asymptotic formula (32). For the elliptic cylinder $x^2/b^2 + y^2/a^2 = 1$, we have $|D| = \pi ab$, $m_{xx} = \rho \pi a^2$ and (41) gives

$$\tilde{F}_x(0) = \frac{b}{a} + 1 = 2 - \frac{1}{2}e^2 - \frac{1}{8}e^4 + \mathcal{O}(e^6),$$

which corresponds to the asymptotic formula (33).

For the square cylinder with side $2a$, we have $|D| = 4a^2$ and $m_{xx} \approx 1.51\rho\pi a^2$, which gives

$$\tilde{F}_x(0) \approx \frac{4}{\pi} + 1.51 \approx 2.7832.$$

The fifth-order approximation of the section "Hydrodynamic Force on Square Vertical Cylinder" with four terms in the series (34) gives $|\tilde{F}_x(0)| \approx 2.736$ and just one term in the series (34) gives $|\tilde{F}_x(0)| \approx 2.563$. The latter value is close to that predicted by the theory of "equivalent circular radius", see Figure 4. Therefore, the theory by Mogridge and Jamieson (1976) underpredicts the force for long waves by about 8.5%.

## CONCLUSION

An asymptotic approach to the linear problem of regular water waves interacting with a vertical cylinder of arbitrary cross section has been presented. The incident regular wave is one-dimensional, water is of finite depth, and the rigid cylinder extends from the bottom to the water surface. Deviation of the cylinder surface from a mean circular cylinder is assumed small compared with the radius of the mean circular cylinder. The fifth-order asymptotic solution of the problem has been obtained. Each term in the asymptotic expansion of the velocity potential is the solution of a radiation problem for the circular cylinder. These radiation problems differ only by the value of the normal derivative of the corresponding potential on the surface of the circular cylinder. The radiation problems have been solved by the Fourier method. The numerical solution of the problem has been reduced to operations with the Fourier coefficients of the potentials and the shape function. The numerical algorithm has been applied to the problems of wave diffraction by elliptic, square and quasi-elliptic cylinders and by the cylinder with cosine type radial perturbation. The obtained results have been compared with experimental and numerical results by others in terms of the hydrodynamic forces and wave runup on cylinders in waves. The present approach provides the forces very close to the forces computed numerically and measured in experiments for relatively long incident waves, $0 < kR < 4$, where $2\pi/k$ is the wave length of the incident wave. The present approach should be used with care for short incident waves. A reason for this conclusion comes from the body boundary condition. The analysis of the velocity potentials $\phi_n$ revealed that they have terms with factors $(kR)^{2n}$. Correspondingly, the expansion (15) is formally asymptotic only if $\varepsilon(kR)^2 \ll 1$. For small values of $\varepsilon$ and short waves with $\lambda/R = \mathcal{O}(\varepsilon^{1/2})$, the method of renormalization or multi-scale method can be used to derive uniformly valid asymptotic expansions of the hydrodynamic forces.

The asymptotic method of this paper has been validated for the long-wave approximation. The long-wave approximation provides the forces acting on a vertical cylinder of arbitrary cross section in linear regular waves through the area of the cylinder cross section and the added masses of this cross section. The values of the forces at $kR = 0$ are exact within the linear wave theory. The added mass tables can be used to calculate the forces at $kR = 0$.

An advantage of the present approach compared with the numerical solution of the problem by a boundary-element method is that it provides the forces and the diffracted wave field in terms of the Fourier series of the deviation of the cylinder shape from the circular one. The leading-order potential, $\phi_0(r,\theta)$, is independent of these coefficients, the first-order potential, $\phi_1(r,\theta)$, is a linear form of these coefficients, and the second-order potential $\phi_2(r,\theta)$ is a quadratic form of the coefficients. By using these forms of the potentials $\phi_n(r,\theta)$, we can formulate the problem of identification of the cylinder and its shape with the help of measured elevations of water surface far from the cylinder. We can also determine how much some small variations of a cylinder shape change the loads acting on this cylinder in waves, and optimize the shape of the cylinder to approach certain restrictions on the loads.

It was found that cylinders with quasi-elliptic cross section experience the least wave force compared with cylinders of elliptic, square and circular cylinders with the same cross sectional area for zero angle of wave incidence, see Figure 7.

In real applications, cylinders are always arranged in groups, therefore the analysis of the so-called ”hydrodynamic interaction problem” of several non-circular cylinders in waves should be carried out. The present method is very suitable for analysis of this problem and it is suggested to solve by iterations satisfying the boundary condition on each cylinder one after another and employing the addition theorem of the Bessel functions. The iterations are suggested to combine with the asymptotic approach of the present paper, in order to improve the convergence of the iterations.

## ACKNOWLEDGEMENT

Preliminary results of this paper were reported at IWWWFB, 2015 (see, Disibuyuk and Korobkin (2015)). This research was started while the first author was visiting the School of Mathematics, University of East Anglia as a visiting research scientist during the period from October 2014 to February 2015. This visit was supported by YÖK (Council of Higher Education of Turkey). The first author was also supported by a grant (BİDEB-2211) from TÜBİTAK (The Scientific and Technological Research Council of Turkey). These supports are greatly acknowledged. The authors would like to thank the reviewers for their suggestions.

## REFERENCES

Au, M. C. and Brebbia, C. A. (1983). “Diffraction of water waves for vertical cylinders using boundary elements.” *Appl. Math. Modelling*, 7(2), 106–114.

Black, J. L., Mei, C. C., and Bray, M. C. G. (1971). “Radiation and scattering of water waves by rigid bodies.” *J. Fluid Mech.*, 46(1), 151–164.

Chen, H. S. and Mei, C. C. (1971). “Scattering and radiation of gravity waves by an elliptical cylinder.” *Report No. 140*, Parsons Lab., Dept. of Civ. Engrg., M.I.T.

Chen, H. S. and Mei, C. C. (1973). “Wave forces on a stationary platform of elliptical shape.” *Journal of Ship Research*, 17(2), 61–71.

De Vos, L., Frigaard, P., De Rouck, J. (2007). “Wave run-up on cylindrical and cone shaped foundations for offshore wind turbines.” *Coastal Engineering*, (54)1, 17–29.

Disibuyuk, N. B. and Korobkin, A. A., (2015). “Wave forces on a vertical cylinder with non-circular cross section.” *30th International Workshop On Water Waves And Floating Bodies, Proceedings*, 53–56.

Eatock Taylor, R. and Hu, C. S. (1991). “Multipole expansions for wave diffraction and radiation in deep water.” *Ocean Engineering*, 18(3), 191–224.

Eatock Taylor, R. and Hung, S. M. (1987). "Second order diffraction forces on a vertical cylinder in regular waves." *Applied Ocean Research*, 9(1), 19–30.

Fichtenholtz, G. M. (2001). *Course of differential and integral calculus*, Vol. 3. Fizmatlit, Moscow. (in Russian).

Garrett, C. J. R. (1971). "Wave forces on a circular dock." *Journal of Fluid Mechanics*, 46(1), 129–139.

Haskind, M. D. (1973). *Hydrodynamic theory of ship rolling*. Fizmatlit, Moscow. (in Russian).

Havelock, T. H. (1940). "The pressure of water waves upon a fixed obstacle." *Proceedings of The Royal Society A*, 175(963), 409–421.

Hwang, L.-S. and Tuck, E. O. (1970). "On the oscillations of harbours of arbitrary shape." *J. Fluid Mech.*, 42(3), 447–464.

Iafrati, A. and Korobkin, A. A. (2006). "Breaking wave impact onto elastic wall." *Proc. 4th Intern. Conference on Hydroelasticity in Marine Technology, Wuxi, China.* 139–148.

Isaacson, M. (1978). "Vertical cylinders of arbitrary section in waves." *Journal of the Waterway, Port, Coastal and Ocean Division*, 104(3), 309–324.

Korobkin, A. A. (2008). "Wagner theory of steep wave impact." *Proc. 23rd Intern. Workshop on Water Waves and Floating Bodies, Jeju, Korea.*, 112–115.

Korobkin, A. A. and Malenica, S. (2007). "Steep wave impact onto elastic wall." *Proc. 22nd Intern. Workshop on Water Waves and Floating Bodies, Plitvice, Croatia.*, 4pp.

Liu, J., Guo, A. and Li, H. (2016). "Analytical solution for the linear wave diffraction by a uniform vertical cylinder with an arbitrary smooth cross-section." *Ocean Engineering*, 126, 163–175.

Lykke Andersen, T., Frigaard, P., Damsgaard, M.L., De Vos, L. (2011). "Wave run-up on slender piles in design conditions - Model tests and design rules for offshore wind." *Coastal Engineering*, 58, 281–289.

MacCamy, R. C. and Fuchs, R. A. (1954). "Wave forces on piles: A diffraction theory." *Report No. 69*, U.S. Army Corps of Engineers, Beach Erosion Board, Washington, D.C.

Mansour, A. M., Williams, A. N., and Wang, K. H. (2002). "The diffraction of linear waves by a uniform vertical cylinder with cosine-type radial perturbations." *Ocean Engineering*, 29(3), 239–259.

Mei, C. C., Stiassnie, M., and Yue, D. K.-P. (2005). *Theory and applications of ocean surface waves. Part 1: Linear aspects*, Vol. 23 of *Advanced Series on Ocean Engineering*. World Scientific Publishing Co. Pte. Ltd., Hackensack, NJ.

Mogridge, G. R. and Jamieson, W. W. (1976). "Wave forces on square caissons." *Proc. 15th Coastal Eng. Conf., ASCE, Chapter 133*, 2271–2289.

Thorne, R. C. (1953). "Multipole expansions in the theory of surface waves." *Math. Proc. Cambridge Philos. Soc.*, 49(4), 707–716.

Ursell, F. (1950). "Surface waves on deep water in the presence of a submerged circular cylinder I." *Math. Proc. Cambridge Philos. Soc.*, 46(1), 141–152.

Wang, Y., Ren, X., Dong, P., and Wang, G. (2011). "Three-dimensional numerical simulation of wave interaction with perforated quasi-ellipse caisson." *Water Science and Engineering*, 4(1), 46–60.

Williams, A. N. (1985). "Wave forces on an elliptic cylinder." *Journal of Waterway, Port, Coastal, and Ocean Engineering*, 111(2), 433–449.

Wrobel, L. C., Sphaier, S. H., and Esperança, P. T. T. (1985). "Propagation of surface waves." *Topics in boundary element research, Vol. 2*, Springer, Berlin, 156–190.

Wu, X.-J. and Price, W. G. (1991). "Evaluation of wave drift forces on vertical cylinders of arbitrary geometry, with application to tension leg platforms (TLPs)." *Ocean Engineering*, 18(1), 1–15.

Yeung, R. W. (1981). "Added mass and damping of a vertical cylinder in finite-depth waters." *Applied Ocean Research*, 3(3), 119–133.

Zhu, S. and Moule, G. (1994). "Numerical calculation of forces induced by short-crested waves on a vertical cylinder of arbitrary cross-section." *Ocean Engineering*, 21(7), 645–662.